

https://dspace.org/

Modulation of cell death and pathogenicity by eugenol tosylate congeners in Candida Albicans

Lone, Shabir Ahmad

2020
https://hdl.handle.net/10539/29949

Downloaded from a DSpace repository. https://dspace.org/

Inhibition of ergosterol synthesis in *Candida albicans* by novel Eugenol Tosylate Congeners targeting sterol 14α-demethylase (CYP51) enzyme

Originally published under terms of the Creative Commons Attribution 4.0 International License, in: Archives of Microbiology, 2020;202(4):711-726. doi: 10.1007/s00203-019-01781-2.

Archives of Microbiology (2020) 202:711–726
https://doi.org/10.1007/s00203-019-01781-2

ORIGINAL PAPER

Inhibition of ergosterol synthesis in *Candida albicans* by novel eugenol tosylate congeners targeting sterol 14α-demethylase (CYP51) enzyme

Shabir Ahmad Lone[1] · Shama Khan[1] · Aijaz Ahmad[1,2]

Received: 29 September 2019 / Revised: 13 November 2019 / Accepted: 20 November 2019 / Published online: 30 November 2019
© Springer-Verlag GmbH Germany, part of Springer Nature 2019

Abstract

This study is a continuation and extension of our previous study in which we synthesized seven novel eugenol tosylate congeners (ETC-1 to ETC-7) from a natural compound eugenol and checked their antifungal activity against different isolates of *Candida albicans*. All these ETCs showed potent antifungal activity to varying degrees. In this study, the aim is to evaluate the effect of most active compounds (ETC-5, ETC-6 and ETC-7) on ergosterol biosynthesis pathway and cellular viability in *C. albicans* by applying combined approach of in silico and in vitro methodologies. In silico studies were done through all atom molecular mechanics approach and free binding energy estimations, and in vitro study was done by estimating total intracellular sterol content and effect on expression of *ERG11* gene. Furthermore, effect on cell viability by these compounds was also tested. Our results demonstrated that these ETCs target ergosterol biosynthesis pathway in *C. albicans* by inhibiting the lanosterol 14-α demethylase enzyme and also downregulates expression of its related gene *ERG11*. Furthermore, these ETCs exhibit potent fungicidal effect in cell viability assay, thus overall results advocating the claim that these tosylates have potential to be taken to next level of antifungal drug development.

Keywords Eugenol tosylates congeners · *C. albicans* · Ergosterol · Molecular docking

Introduction

Globally, *Candida* species are the second and fifth most common causative agents for fungal and nosocomial infections, respectively (Brown et al. 2012; Sievert et al. 2013). Around 600 fungal species, including over 20 *Candida* species, are known to be human pathogens (Piccione et al. 2019). Among these, *C. albicans* is the most predominant and most isolated species (Lindberg et al. 2019). Although they are commensals, they become pathogenic with the host immunocompromised conditions. The disease spectrum of candidiasis ranges from localised superficial to systemic candidemia. Currently, there is limited number of antifungal drugs available as compared to antibacterial drugs. The major classes of antifungal drugs, based on their mechanism of action are azoles, polyenes, allylamines, echinocandins and fluoropyrimidines. Most widely used drugs for antifungal therapy used ergosterol biosynthesis pathway or its end product ergosterol for their target. The antifungal drugs including azoles, polyenes, allylamines, thiocarbamates and morpholines using ergosterol as their target (Rajput and Karuppayil 2013). Most of these existing antifungals are associated with high toxicity, severe adverse side effects and emerging multiple drug resistance. Based on these facts, there is a need for exploring safer alternatives.

Natural products have long been known to possess antimicrobial activities and is a source of new drugs (Dias et al. 2012). Currently, synthesizing derivatives/analogues from products of natural origin by applying medicinal chemistry are of great scientific focus. Eugenol (4-allyl-1-hydroxy-2-methoxybenzene) is one of the extensively studied natural product for its pharmacological actions. Various studies

Communicated by Erko Stackebrandt.

Electronic supplementary material The online version of this article (https://doi.org/10.1007/s00203-019-01781-2) contains supplementary material, which is available to authorized users.

✉ Aijaz Ahmad
Aijaz.Ahmad@wits.ac.za; Aijaz.Ahmad@nhls.ac.za

[1] Clinical Microbiology and Infectious Diseases, School of Pathology, Health Sciences, University of the Witwatersrand, Johannesburg 2193, South Africa

[2] Infection Control, Charlotte Maxeke Johannesburg Academic Hospital, National Health Laboratory Service, Johannesburg 2193, South Africa

have already been reported antifungal activity of eugenol and its derivatives (Carrasco et al. 2012; Ahmad et al. 2015; Hipólito et al. 2018; da Silva et al. 2018). In our previous study, potent antifungal activity of different eugenol tosylate derivatives have been reported (Ahmad et al. 2015). Our previous findings also revealed that eugenol and its derivatives inhibit ergosterol biosynthesis (Ahmad et al. 2010, 2015). Based on these studies, we further used eugenol as a parent source to synthesize eugenol tosylate congeners (ETCs) with different functional groups and assuming better and improved antifungal activity against different fluconazole-susceptible and resistant *C. albicans* strains.

In this study, all seven newly synthesized eugenol tosylate congeners (ETC-1 to ETC-7) were docked using the concepts of combinatorial chemistry and the top three inhibitors—ETC-5, ETC-6 and ETC-7—were filtered based on the most promising binding energies against CYP51 protein (*ERG11*). These top three generated complexes were further analysed using 50 ns Molecular Dynamic (MD) simulations in explicit solvent conditions and their conformational behaviours were analyzed. Furthermore, we investigated the effect of three most active newly synthesized eugenol tosylate congeners (ETC-5, ETC-6 and ETC-7) on cell viability and ergosterol biosynthesis pathway by quantifying the total intracellular sterol content. We have checked the effect on expression of *ERG11* gene, which is related to ergosterol biosynthesis pathway by RT-qPCR.

Materials and methods

Candida strains and eugenol tosylate congeners

In this study, three *C. albicans* isolates were used comprising of one clinical fluconazole-susceptible, one clinical fluconazole-resistant and one laboratory control strain *C. albicans* SC5314 (ATCC MYA-2876). The clinical isolates were collected from patients visiting Charlotte Maxeke Johannesburg Academic Hospital. The ethical clearance number M000402 obtained from the Human Research Ethics Committee, University of the Witwatersrand was used for these isolates. The isolates were stored at − 80 °C supplemented with 20% glycerol in the Department of Clinical Microbiology and Infectious Diseases, University of the Witwatersrand, Johannesburg until required. All culture media and other chemicals used in this study were of high analytical grade.

Seven novel eugenol tosylate congeners were synthesized by tosylating eugenol on the hydroxyl group as detailed in our previous study and their antifungal susceptibility was determined against 11 *C. albicans* strains (Ahmad et al. 2015; Lone et al. 2019 under review). In continuation with these studies, most potent antifungal compounds (ETC-5, ETC-6 and ETC-7) were selected in this study to determine the effect of these compounds on ergosterol biosynthesis pathway.

In silico methodology

Preparation of initial systems

An initial X-ray crystallographic structures of lanosterol 14-alpha demethylase –cytochrome P451 enzyme (CYP451, PDB code: 5V5Z) was retrieved from the Protein Data Bank (PDB) database (Berman et al. 2000; Keniya et al. 2018). A series of seven compounds were used in this study and all the compounds were prepared using MarvinSketch 6.2.1, 2014, ChemAxon (https://www.chemaxon.com) and Molegro Molecular Viewer (MMV) was used to ensure the geometry and hybridization state. The prepared system's protonation states were optimized and hydrogens were added with the Protein Preparation Wizard in Maestro software (Sastry et al. 2013).

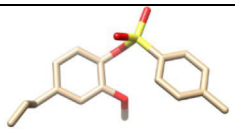
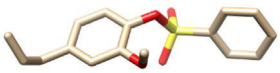
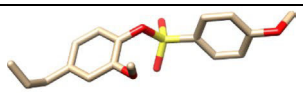
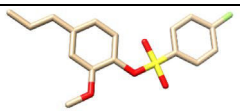
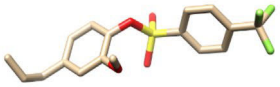
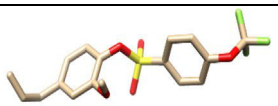
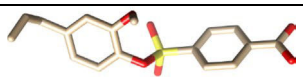
Molecular docking studies

All seven compounds, ETC-1, ETC-2, ETC-3, ETC-4, ETC-5, ETC-6 and ETC-7 (Table 1), were chosen to dock at the CYP51 active site along with HEME (Fig. 1), as this metal ion plays important role in the binding of inhibitors (Keniya et al. 2018). Autodock Vina tool was used to perform the docking studies of the inhibitors with protein (Trott and Olson 2010). The process was run with default parameters of the software. The grid box size and center parameters for CYP51 were x (− 40,14) y (− 11,14) and z (24,14), respectively. Based on the highest binding energy and previously determined minimum inhibitory concentrations, ETC-5, ETC-6 and ETC-7 compounds were chosen for further studies. Then, complex was prepared using Chimera tool (Pettersen et al. 2004) and afterwards subjected to molecular dynamic simulations.

Molecular dynamic (MD) simulations

All three systems were exposed to MD simulation using Graphics Processing Unit (GPU) version of PMEMD package in Amber-18 to define the binding effect on inhibitors selectivity. Termini of the protein chain were capped with neutral residues (acetyl and methylamide) to ensure protein stability during simulation period. The Antechamber module implemented in Amber-18 was used to parametrize the inhibitors and also assign atom types and partial charges. To define a protein, AMBER forcefield FF14SB was applied (Perez et al. 2015). Missing hydrogens and counter ions for system neutralization

Table 1 List of generated binding energies of the docked ligands in complex with CYP51 protein

Compound	Ligand name	Ligand structure (3D)	Binding energy (Kcal/mol)	MIC* (µg/ml)
ETC-1	4-allyl-2-methoxyphenyl 4-methylbenzenesulfonate		-8.9	16 – 128
ETC-2	4-allyl-2-methoxyphenyl benzenesulfonate		-8.4	32 – 256
ETC-3	4-allyl-2-methoxyphenyl 4-methoxybenzenesulfonate		-8.6	64 – 512
ETC-4	4-allyl-2-methoxyphenyl 4-fluorobenzenesulfonate		-8.7	16 – 128
ETC-5	4-allyl-2-methoxyphenyl 4-(trifluoromethyl) benzene		-9.1	0.125 – 1.0
ETC-6	4-allyl-2-methoxyphenyl 4-(trifluoromethoxy) benzene		-9.5	0.25 – 2.0
ETC-7	4-((4-allyl-2 methoxyphenoxy) sulfonyl) benzoic acid		-9.0	1 – 8

*Minimum inhibitory concentrations are based on our previous findings

were added to the protein using LEaP module of Amber-18. TIP3P water box was included in the corresponding complexes by maintaining the distance of 10 Å among the solute atom and surface (Spoel and Maaren 2006). Periodic boundary state was implemented using particle mesh Ewald (PME) method of Amber-18 by direct space and van der Waals cut-off of 10 Å (Harvey and Fabritiis 2009). A 2-fs integration time step was used for the simulations. Before MD simulations, system minimization was conducted with restraint potential of 10 Å to consider the solute molecule using steepest descent 500 steps, followed by steps of 1000 conjugate gradient minimization process. Afterwards, complexes were slowly thermalized from 0 to 300 K through the harmonic restrains of 10 Å to keep the solute atoms static. For temperature regulation, Langevin thermostat was used with a collision random frequency of 1.0 ps. Equilibration of the systems were performed for 5-ns at 300 K, while maintaining constant pressure at 1 bar with Berendsen barostat. The SHAKE algorithm was implemented to confine hydrogen bonds. Finally, 50 ns production phase runs were performed to analyze the motions in the trajectory. Root Mean Structure Dynamics (RMSD), Root Mean Structure Fluctuation (RMSF), Radius of Gyration (RoG) and MMGBSA were calculated using CPPTRAJ and PTRAJ modules of Amber-18 package (Roe and Cheatham 2013). All plots and visualizations of the trajectories were analyzed using Origin data analysis tool and Maestro Schrödinger software (Sastry et al. 2013).

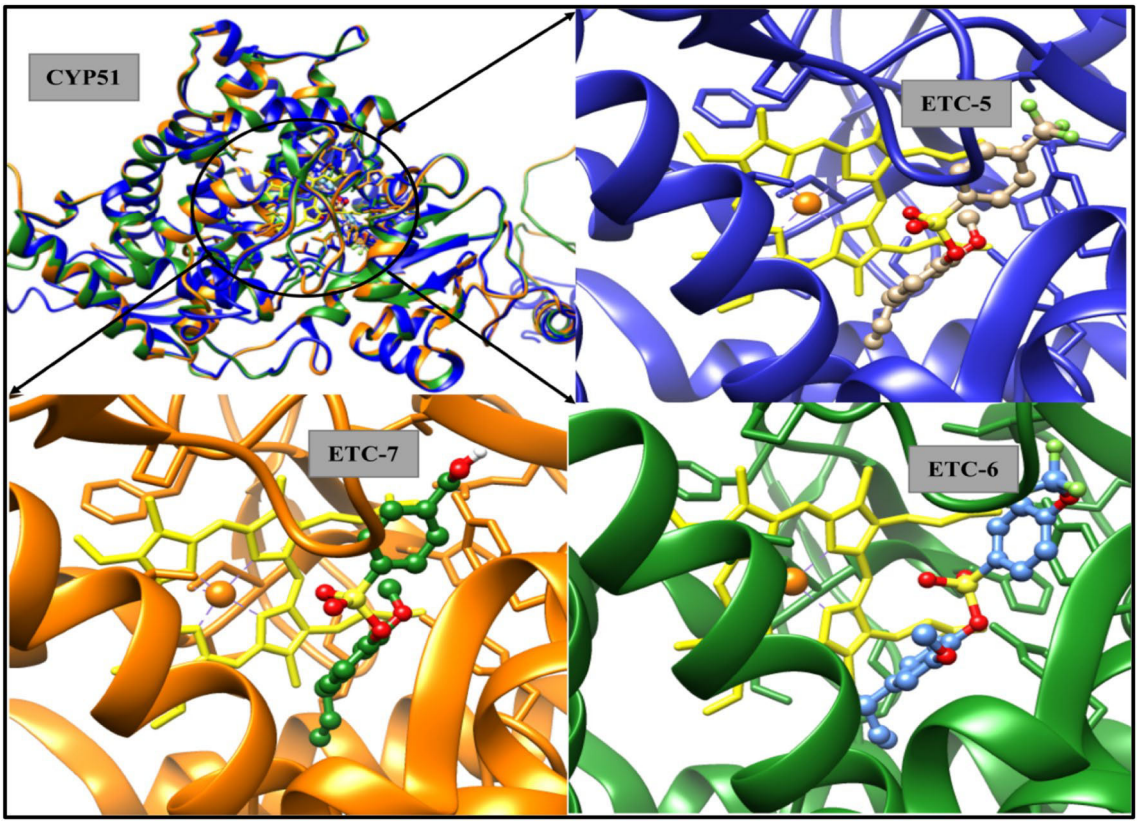


Fig. 1 CYP51 protein (superimposed; blue, green and orange color) in complex with HEME; ETC-5, ETC-6 and ETC-7. Yellow color represents HEME metal ion and grey, light blue and green color represents ETC-5, ETC-6 and ETC-7 inhibitors respectively (color figure online)

In vitro methodology

Ergosterol biosynthesis assay

The effect of ETCs on ergosterol synthesis in *C. albicans* cells was determined using a method described previously (Ahmad et al. 2011). Briefly, *C. albicans* cells were inoculated in 50 ml of Sabouraud Dextrose Broth with different concentrations of test compounds and incubated for 18 h with shaking at 37 °C. Following incubation, cells were harvested by centrifugation at 2700 rpm × 5 min, washed and weighed. Each pellet then treated with 3 ml of freshly prepared alcoholic potassium hydroxide solution (25%) and vortexed for 1 min. Cell suspensions were then incubated for 1 h at 85 °C in water bath. After incubation, the tubes were allowed to cool. Sterols were then extracted by the addition of water (1 ml) and *n*-heptane (3 ml) mixture followed by vortexing for 3 min. Analysis was done by diluting 1 mL aliquot of sterol extract with fivefold in 100% ethanol and scanned spectrophotometrically between 240 and 300 nm using UV-1800 SHIMADZU spectrophotometer (Shimadzu Corporation, Japan). Untreated cells and cells treated with 8 µg/ml of fluconazole were used as negative and positive controls, respectively. The ergosterol content was calculated as a percentage of the wet weight of the cell by the following equation:

$$\%\text{Ergosterol} + \%24(28)\text{DHE} = \frac{\left[\left(\frac{A281.5}{290}\right) \times F\right]}{\text{Pellet weight}},$$

$$\%24(28)\text{DHE} = \frac{\left[\left(\frac{A230}{518}\right) \times F\right]}{\text{Pellet weight}},$$

$$\%\text{Ergosterol} = \left[\%\text{ergosterol} + \%24(28)\text{DHE}\right] - \%24(28)\text{DHE},$$

where F is the factor for dilution in ethanol, 290 and 518 are the E values (in percentages per centimetre) determined for crystalline ergosterol and 24 (28) DHE, respectively.

Gene expression

To study the effect of synthesized tosylates on the gene expression of ergosterol biosynthesis genes, real-time PCR was performed using method described by (Ahmad et al. 2015) with modifications. Briefly, *C. albicans* cells were sub-cultured in 10 ml of SD broth to give a final

concentration of 5 × 106 cells/ml, followed exposure to MIC value of the test compounds and incubated at 37 °C for 3 h. Cells without drugs were used as negative control. Total RNA was isolated using Quick-RNA Fungal/Bacterial Miniprep Kit (Zymo Research, CA, USA) following the manufacturer's instructions. Concentration of total RNA was measured using Nanodrop 2000 spectrophotometer (Thermo Scientific). The cDNA was synthesized using iScript™ cDNA synthesis kit (Bio-Rad, CA, USA) according to manufacturer's instructions. Three housekeeping genes (ACT1, PMA1 and RPP2B) were used as reference controls. The relative expressions of the gene ERG11 was determined using reverse transcription quantitative polymerase chain reaction (RT-qPCR) using PowerUpTM SYBRTM Green Master Mix (2X) (Thermo Fisher Scientific, MA, USA). Primers for above-mentioned genes were designed using NCBI/Primer 3-Blast and are presented in Table 2. The thermal cycling conditions for all RT-qPCR amplifications were UDG activation at 50 °C for 2 min, initial denaturation at 95 °C for 2 min, denaturation (40 cycles) at 95 °C for 15 s, annealing at 50 °C for 60 s and extension at 72 °C for 60 s. Amplifications were performed using the RocheLight® Cycler Nano instrument (Roche, Basel, Switzerland).

Furthermore, efficiency of the amplifications was confirmed by analysing the standard curves of both the genes of target and housekeeping genes. Fold difference was calculated using the formula $2 - (\Delta\Delta Ct)$, where ΔCt was the mean Ct value of the target gene minus the mean of housekeeping genes, and ΔΔCt was the ΔCt of the tested cells minus ΔCt of the control cells.

Cell viability assay

Cell viability assay was done using Muse Count and Viability kit (EMD Millipore, USA) according to the manufacturer's instructions. This technique allows quantitative analysis of cell viability by differentially staining live and dead cells based on their permeability to the dyes present in the reagent. Briefly, *Candida* cells were treated with varying concentrations of test entities and incubated overnight at 37 °C. A uniform cell suspension (1×10^7 cells/ml) was prepared in normal saline, then 20 µl from this suspension were stained with the 380 µl of viability reagent followed by an incubation of 5 min at room temperature in dark. Samples were analyzed by the MUSE cell analyzer (EMD Millipore, Germany). In every set of experiment, heat killed cells and cells without any drug were used as positive and negative controls, respectively.

Statistical analysis

The statistical analysis was performed using Dunnett's multiple comparisons of a two-way ANOVA test by GraphPad Prism 8 software. All the experiments were performed independently in triplicates ($n = 3$), and data were presented as mean ± standard deviation (SD). Values of P (****$P < 0.0001$, ***$P = 0.0009$) were considered as statistically significant.

Results

Structural dynamics and fluctuation

To determine protein stability on the ligand binding, we calculated the root-mean-square dynamics (RMSD) for three systems (Fig. 2). The RMSD is a parameter aimed to compute the aberrations in the conformational stability of macromolecules from the carbon backbone structure to the initial starting structure. The in silico results displayed that CYP51-ETC-5 complex significantly altered the protein conformation as compared to CYP51-ETC-6 and CYP51-ETC-7 system with average values of 2.45 Å, 2.67 Å and 2.97 Å, respectively. These outcomes indicated that complex CYP51-ETC-5 is relatively stable RMSD profile as compared to the other two complexes. In comparison with the complexes of the available drugs, ETC-6 and ETC-7 inhibitors showed higher perturbations indicating the unstable nature of the complexes. Hence,

Table 2 Oligonucleotide primers used for RT-qPCR

Gene	Primer	Sequence (5′–3′)	Amplicon length (bp)	Source
ERG11	Forward	*CTC ATG GGG TTG CCA ATG TT TTT*	207	This study
	Reverse	*GAG CAG CAT CAC GTC TC*		
ACT1	Forward	*TGG TGA TGA AGC CCA ATC CA CAT*	169	This study
	Reverse	*TGG AGC TTC GGT CAA CA*		
PMA1	Forward	*GAA GGT GCT ACT GAT GCT GC GCA*	242	This study
	Reverse	*ACA TCA GCG AAA ATG GC*		
RPP2B	Forward	*ACA CCT CTC CAT CAG CTT CT TGG*	155	This study
	Reverse	*GAC AGA AGC TAA TTT GGT G*		

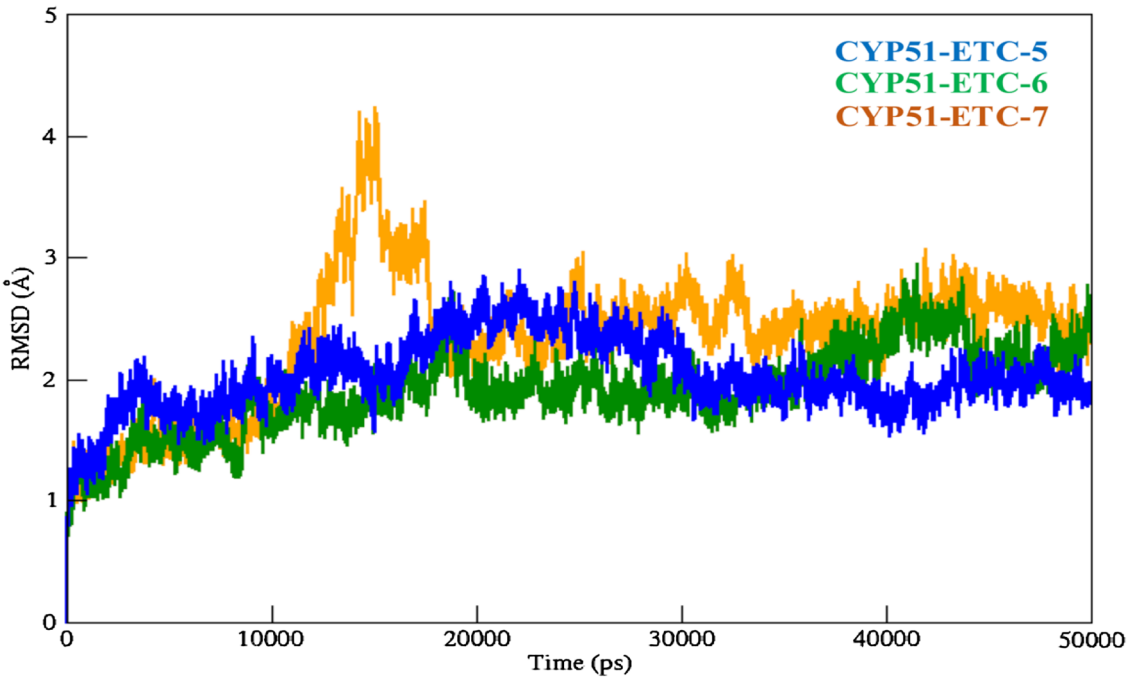


Fig. 2 The curves illustrating the changes in the RMSD values for CYP51-ETC-5, CYP51-ETC-6 and CYP51-ETC-7 complexes over 50,000 ps (50 ns)

CYP51-ETC-5 complex improved the 3D conformation suitable for antifungal activity of ETC-5 inhibitor.

Additionally, to evaluate the inhibitory effects of ETC-5, ETC-6 and ETC-7 of CYP51 targeting, residual fluctuations were calculated by analyzing the root-mean-square fluctuation (RMSF) in carbon backbone atoms. Binding of ETC-6 and ETC-7 ligands considerably disturbed the backbone atoms by producing noteworthy perturbations and residual mobility (Fig. 3). Furthermore, significant fluctuations in the active site residues as induced by the presence of inhibitor could account for the lack of functionality in the ETC-6 and ETC-7 inhibitors as compared to ETC-5 inhibitor.

We also computed Radius of Gyration (RoG) to explore the compactness of the three systems unveiling insights into complex changes in the molecular structure (Fig. 4). With RoG, we investigated the compactness or flexibility of the residues during the simulations time period. The CYP51-ETC-5 complex showed lower RoG over 50 ns simulation, with an average value of 23.61 Å and this suggests the increased stability in the binding of ETC-5 inhibitor. The CYP51-ETC-6 and CYP51-ETC-7 complex displayed higher RoG with an average value of 23.73 Å and 23.98 Å by suggesting a less compact structure when compared to CYP51-ETC-5 system as shown in Fig. 4.

Free binding energy calculations

The Molecular Mechanics/Generalized-Born Surface Area (MM/GBSA) technique is a standard method to calculate the free binding energy of small molecules to biological macromolecules (Genheden and Ryde 2015). This method was used to compute the average binding energy of CYP51-ETC-5, CYP51-ETC-6 and CYP51-ETC-7 complexes as presented in Table 3. Noteworthy alterations in free-binding energies are observed higher (ΔG_{bind} − 36.5278 kcal/mol) in CYP51-ETC-5 complex related to CYP51-ETC-6 (ΔG_{bind} − 33.9182 kcal/mol) and CYP51-ETC-6 (ΔG_{bind} − 32.5297 kcal/mol) complexes, with the better negative value displaying promising binding. The difference in binding energy only differs by ΔG_{bind} − 3.9981 kcal/mol among CYP51-ETC-5 and CYP51-ETC-7 complexes. The van der Waals (ΔE_{vdW}) energy is only showing the difference of − 0.2023 kcal/mol between CYP51-ETC-5 (ΔE_{vdW} − 46.7896 kcal/mol) and CYP51-ETC-7 (ΔE_{vdW} − 46.9919 kcal/mol) complexes; though, it is highest in CYP51-ETC-6 (ΔE_{vdW} − 49.8317 kcal/mol). The electrostatic energy or Coulomb energy is higher in CYP51-ETC-5 complex (ΔE_{ele} − 18.4943 kcal/mol) in contrast with the CYP51-ETC-6 complex (ΔE_{ele} − 16.1096 kcal/mol) and CYP51-ETC-7 (ΔE_{ele} − 5.1190 kcal/mol) by showing major

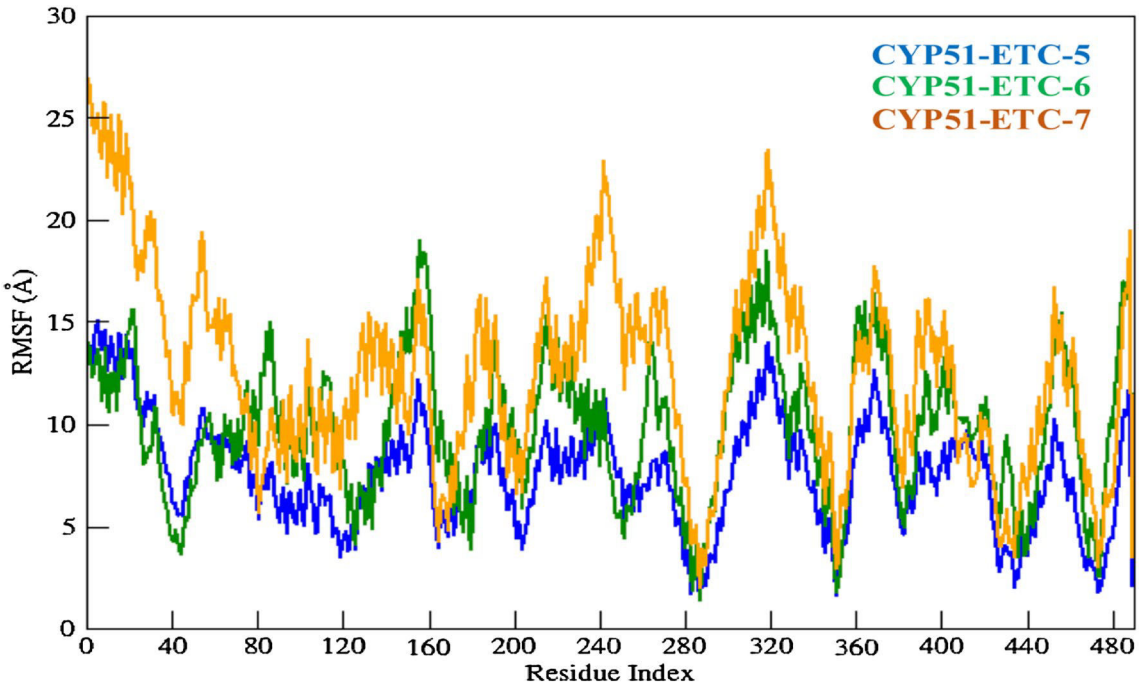


Fig. 3 The graphs showing the alterations observed in residual fluctuations involved in the interaction of CYP51 protein with ETC-5, ETC-6 and ETC-7 inhibitors in the studied complexes

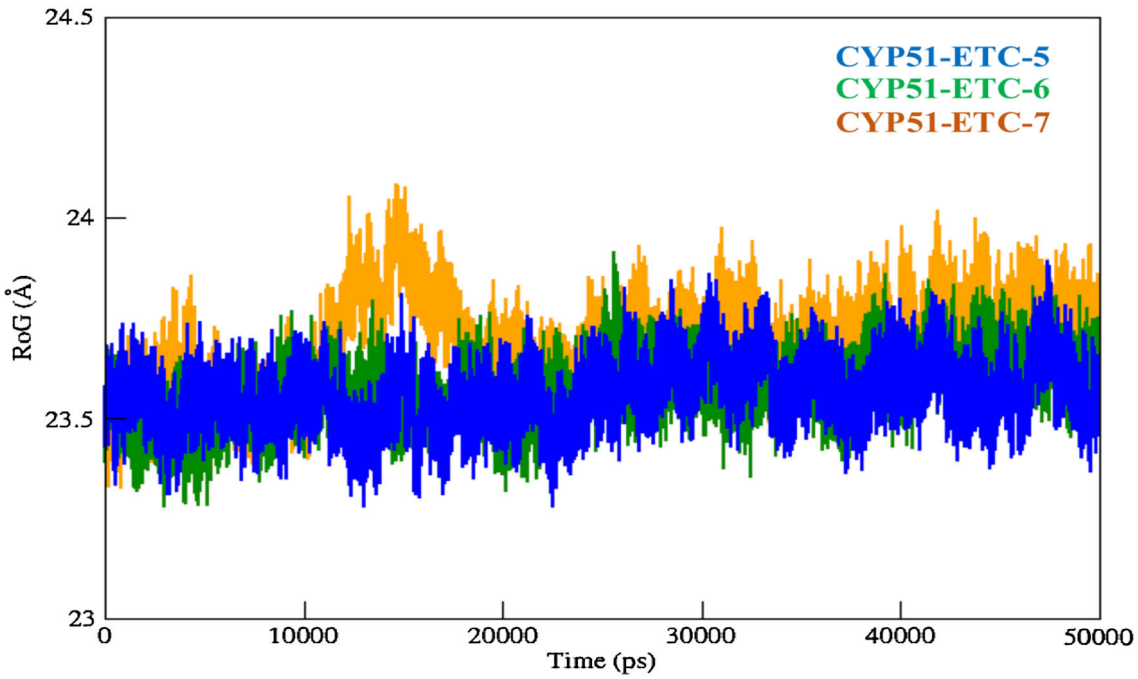


Fig. 4 Comparative compactness (RoG) of ETC-5, ETC-6 and ETC-7 inhibitors of CYP51 protein during 50,000 ps (50 ns)

difference of − 13.3753 kcal/mol, following the pattern of favoring CYP51-ETC-5 complex inhibition.

The gas-phase energy (ΔG_{gas}) is the highest energy calculated in CYP51-ETC-5 complex with the value of − 65.9413 kcal/mol in contrast with other estimated energies of CYP51 protein. The solvation energy is the only energy exhibiting positive value of 28.7534 kcal/mol in CYP51-ETC-5 complex 32.0231 in CYP51-ETC-6 complex and

Table 3 MM/GBSA-based binding free energy profile of CYP51-ETC-5, CYP51-ETC-6 and CYP51-ETC-7 complexes

Complexes	ΔE_{vdW}	ΔE_{ele}	ΔG_{gas}	ΔG_{sol}	ΔG_{bind}
CYP51-ETC-5	−46.7896	−18.4943	−65.9413	28.7534	−36.5278
CYP51-ETC-6	−49.8317	−16.1096	−65.2812	32.0231	−33.9182
CYP51-ETC-7	−46.9919	−5.1190	−52.1109	19.5812	−32.5297

All energies are in kcal/mol

19.5812 kcal/mol in CYP51-ETC-7 complex, thus disapproving to the ligand binding. However, the total binding energy favors the CYP51-ETC-5 complex to inhibit the CYP51 protein. Our findings suggest that altogether ΔE_{ele}, ΔE_{vdW} and ΔG_{gas} define the binding energies of ETC-5 to the active pocket of CYP51 protein.

Furthermore, interaction of amino acid residues comprised in the active site with ETC-5, ETC-6 and ETC-7 was studied to gain the understanding of ligand–protein interactions. The understanding of both ETC-5, ETC-6 and ETC-7 within the active site residues has been shown in Fig. 5. The

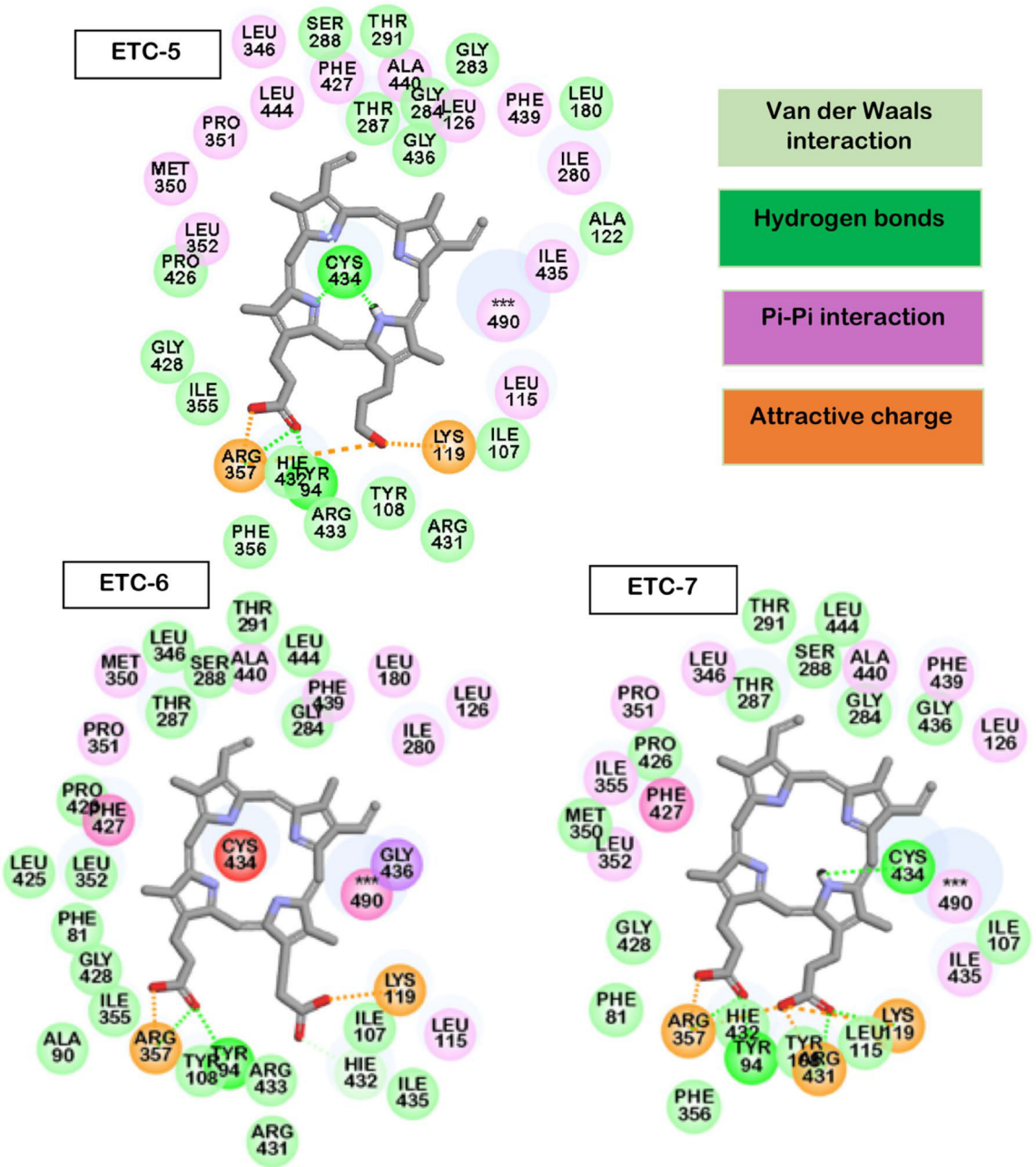


Fig. 5 The key interactions between the active site residues and ETC-5, ETC-6 and ETC-7

carbonyl group of ETC-5 formed two hydrogen bonds with the active site residue Tyr94 and Arg357 with the distance of 1.889 Å and 2.736 Å, respectively. Cys434 amino acid residue is also creating a network of hydrogen bond with ETC-5 inhibitor. Lys119 and Arg357 are positively charged amino acid residues, thus they are attracted towards the ETC-5 inhibitor. The same carboxyl group of ETC-6 inhibitor is contributing in the hydrogen bond network by forming two bonds with Tyr94 and Arg357 individually. ETC-7 inhibitor is forming four hydrogen bonds with active-site amino acid residues Tyr94, Arg431, Lys119 and Cys434. There is no pi–pi interaction in three inhibitors. Hydrogen bond network plays a significant role in the ETC-5, ETC-6 and ETC-7 binding, hence the lack of these bonds among the inhibitor and protein affects the positioning of the ligands and subsequently affects the drug binding.

Ergosterol biosynthesis

The effect of test compounds on ergosterol biosynthesis in various *C. albicans* isolates were studied by quantifying the total intracellular sterols followed method described by (Ahmad et al. 2015) with slight modifications. The ergosterol biosynthesis inhibition and %-age reduction by test entities in different *C. albicans* strains are represented in Figs. 6 and 7, respectively. All the test compounds (ETC-5,

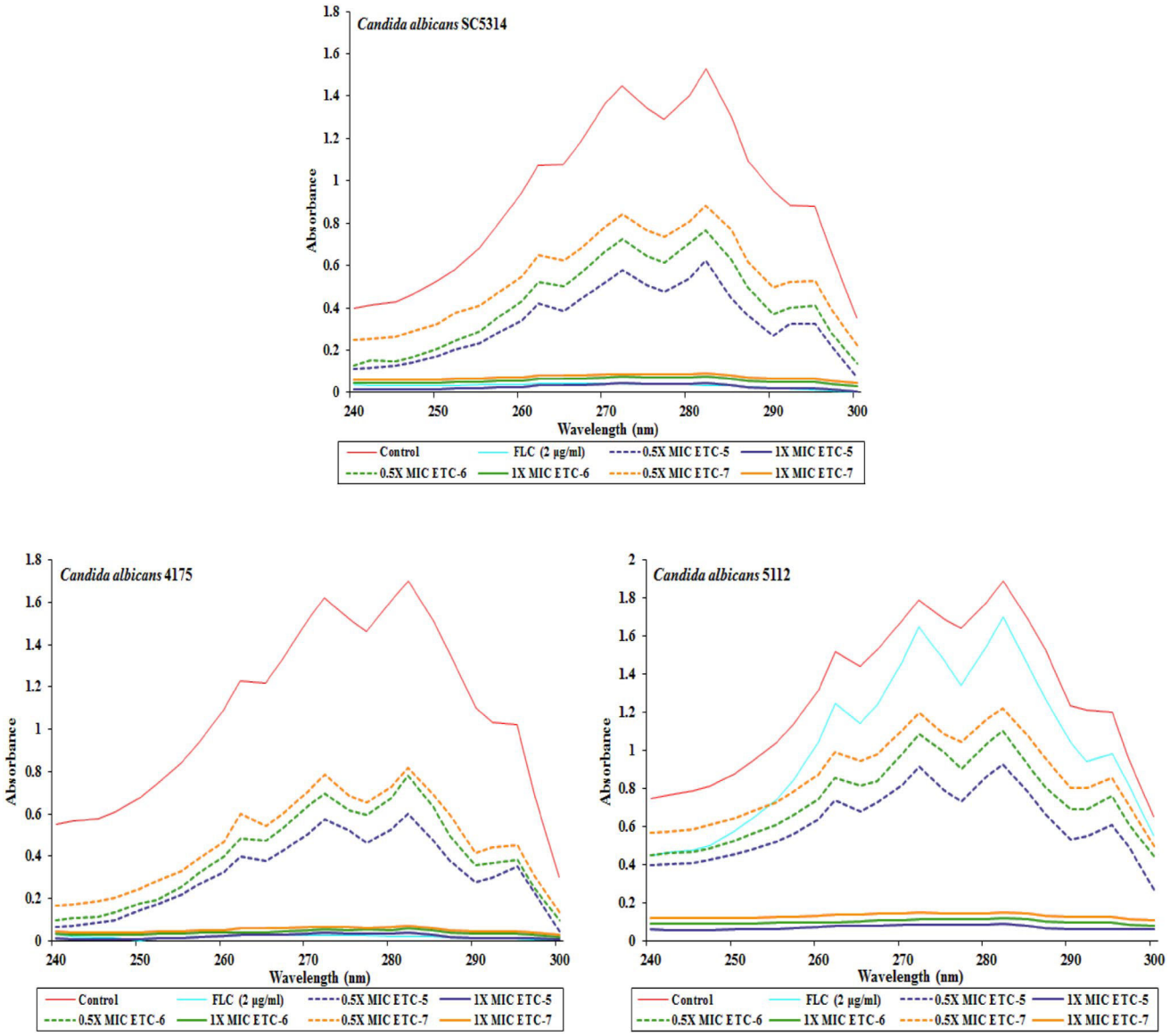


Fig. 6 Effect on ergosterol production in control strain *C. albicans* SC5314, fluconazole-susceptible *C. albicans* 4175 and fluconazole-resistant *C. albicans* 5112 strains after treatment with 0.5×MIC and 1×MIC values of ETC-5, ETC-6 and ETC-7. Untreated cells and cells treated with 8 µg/ml of fluconazole represents negative and positive control, respectively

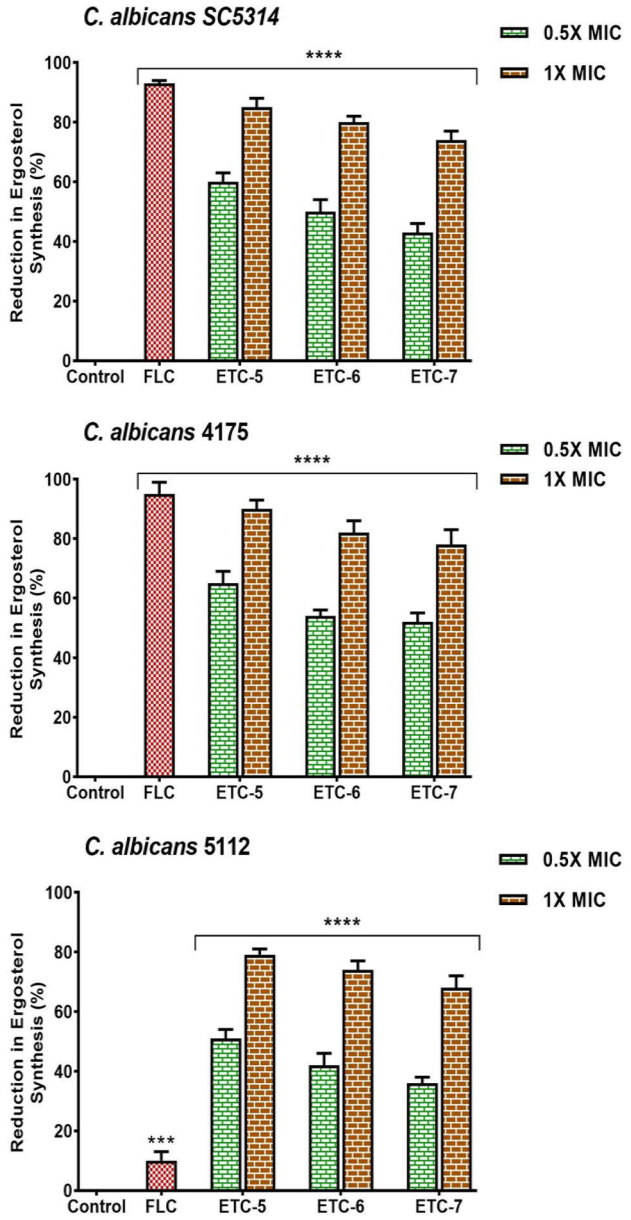


Fig. 7 Percentage of reduction in ergosterol synthesis in control strain *C. albicans* SC5314, fluconazole-susceptible *C. albicans* 4175 and fluconazole-resistant *C. albicans* 5112 strains after treatment with 0.5 × MIC and 1 × MIC values of ETC-5, ETC-6 and ETC-7. Percent reduction in cellular ergosterol content was assessed by compared with that of control cells (untreated cells). Fluconazole (8 µg/ml) represents the positive control. Data are presented from three independent experiments using means ± SD, ****$P < 0.0001$, ***P: 0.0009

ETC-6 and ETC-7) showed significant decrease in ergosterol biosynthesis of *C. albicans* in a dose-dependent manner when compared to untreated control cells. The %-age decrease in ergosterol content at MIC values of test compounds for control strain *C. albicans* SC5314 ranges from 74 to 85% and at 0.5 × MIC the ergosterol content decreases in the range of 43–60%. For fluconazole-susceptible strain *C.*

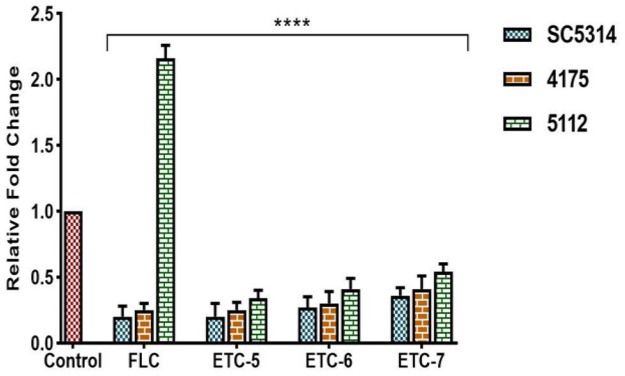


Fig. 8 Relative quantification of *ERG11* gene expression after normalization to housekeeping genes (*ACT1*, *PMA1* and *RPP2B*) in control strain *C. albicans* SC5314, fluconazole-susceptible *C. albicans* 4175 and fluconazole-resistant *C. albicans* 5112 strains after exposed to test compounds (ETC-5, ETC-6 and ETC-7) at their respective MIC values or fluconazole (8 µg/ml). Cells without drugs were used as negative control. Data are presented from three independent experiments using means of fold changes ± SD, ****$P < 0.0001$

albicans 4175, the total ergosterol content decreased in the range 78–90% and 52–65% at MIC and 0.5 × MIC values of the test compounds, respectively. These figures for fluconazole-resistant strain *C. albicans* 5112 at MIC and 0.5 × MIC values of test compounds were in the range of 68–79% and 36–51%, respectively. As expected, the decrease in total ergosterol content by fluconazole (8 µg/ml) in control and fluconazole-susceptible stains of *Candida* were in the range of 93–95%, whereas in fluconazole-resistant strain, only 10% decrease was recorded. ETC-5 showed highest potency to inhibit ergosterol biosynthesis in *C. albicans* cells followed by ETC-6 and ETC-7, respectively.

Gene expression

The effect of test compounds (ETC-5, ETC-6 and ETC-7) at their respective MIC values on ERG11 gene expression in *C. albicans* cells were tested and the results are summarized in Fig. 8. The expression of *ERG11* gene is shown as relative values in comparison to the control (untreated) that were set to one. Our results revealed that the test entities downregulated *ERG11* gene expression in *C. albicans* SC5314 by 2.78—fivefold, in *C. albicans* 4175 by 2.44—fourfold and in *C. albicans* 5112 by 1.85—2.9-fold. The results also showed fluconazole downregulated the *ERG11* gene in *C. albicans* SC5314 and in fluconazole-susceptible *C. albicans* 4175. However, upregulation of *ERG11* gene was observed in fluconazole-resistant *C. albicans* 5112 after exposed to fluconazole (8 µg/ml). ETC-5 exhibited considerable downregulation in expression of *ERG11* gene followed by ETC-6 and ETC-7, respectively.

Viability assay

Based on the in silico results and previously determined MIC values, effect on viability of *C. albicans* cells was determined by Muse Count & Viability kit after treatment of *C. albicans* cells with varying concentrations of test compounds. The viability profile of different *Candida* strains at different concentrations of test compounds are presented in Fig. 9. The results showed that there is a drastic decrease in cell viability and increase in cell death after treatment with test compounds. The

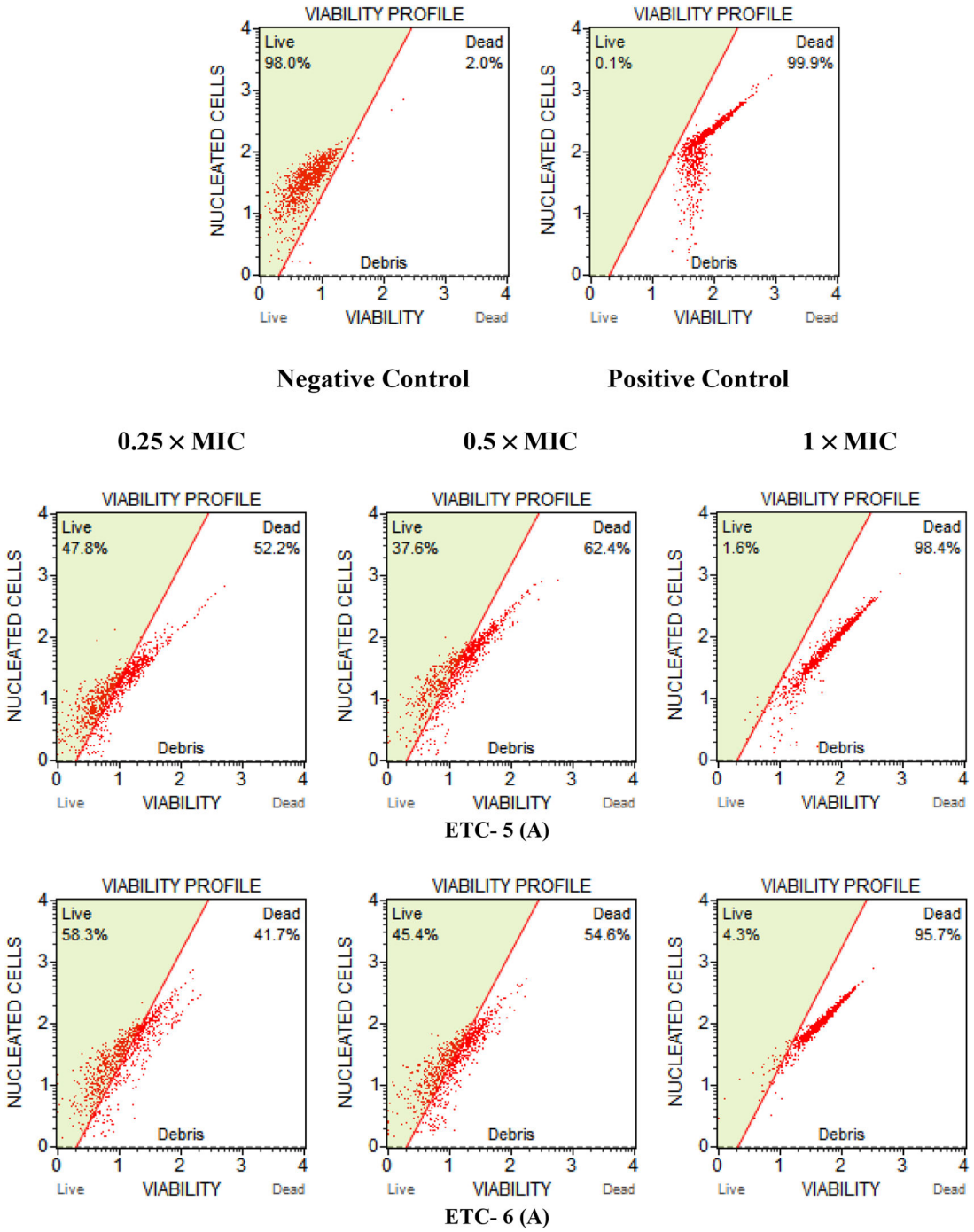


Fig. 9 Cell viability profile of *Candida* cells after overnight treatment to 0.25 × MIC, 0.5 × MIC and 1 × MIC of the test compounds (ETC-5, ETC-6 and ETC-7). **a**–**c** Represents control strain *C. albicans* SC5314, fluconazole-susceptible *C. albicans* 4175, and fluconazole-resistant *C. albicans* 5112 respectively. Percentage live and dead cells are shown in two different subsets. Negative and positive controls represent untreated and heat-killed cells, respectively

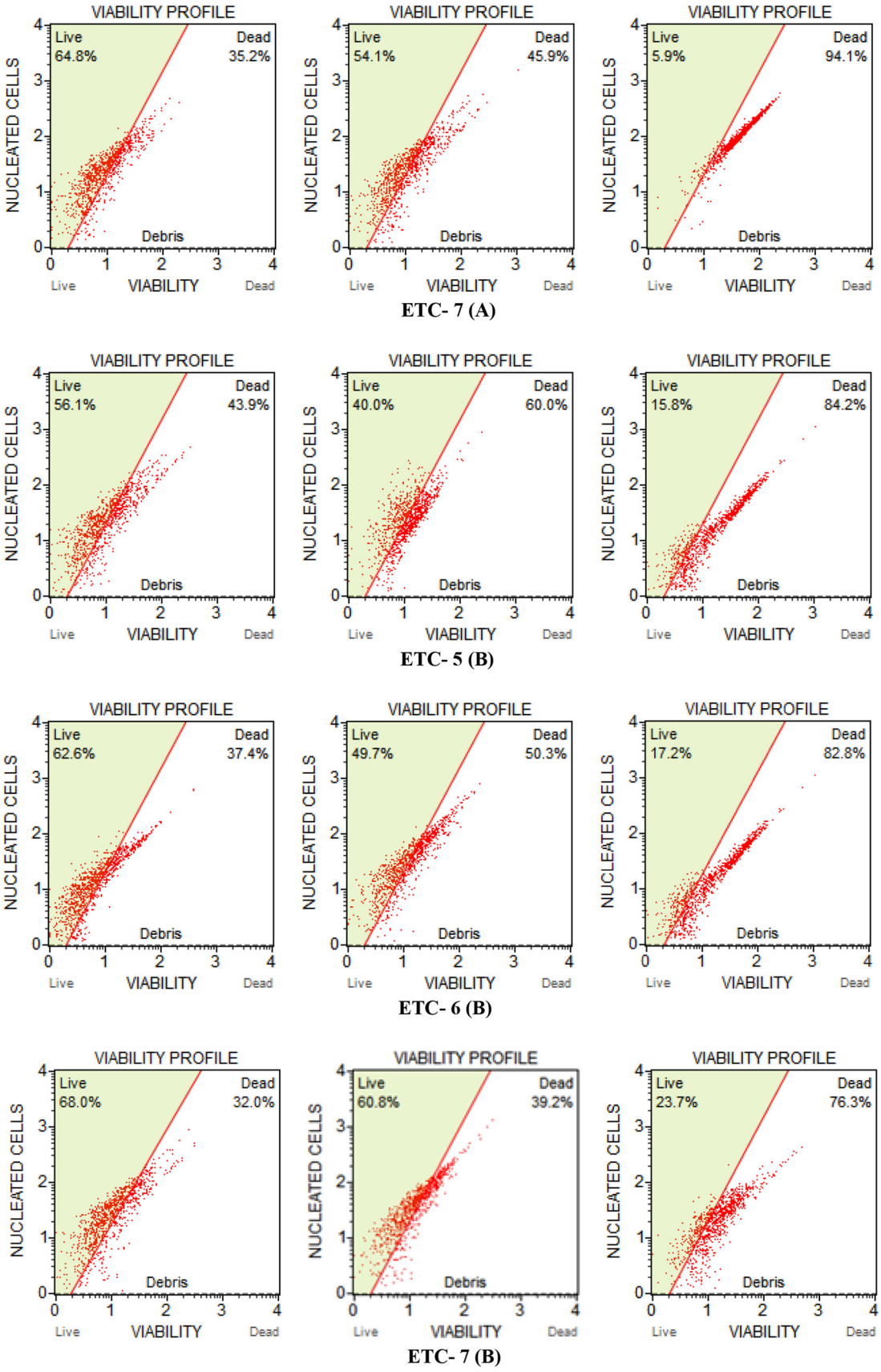


Fig. 9 (continued)

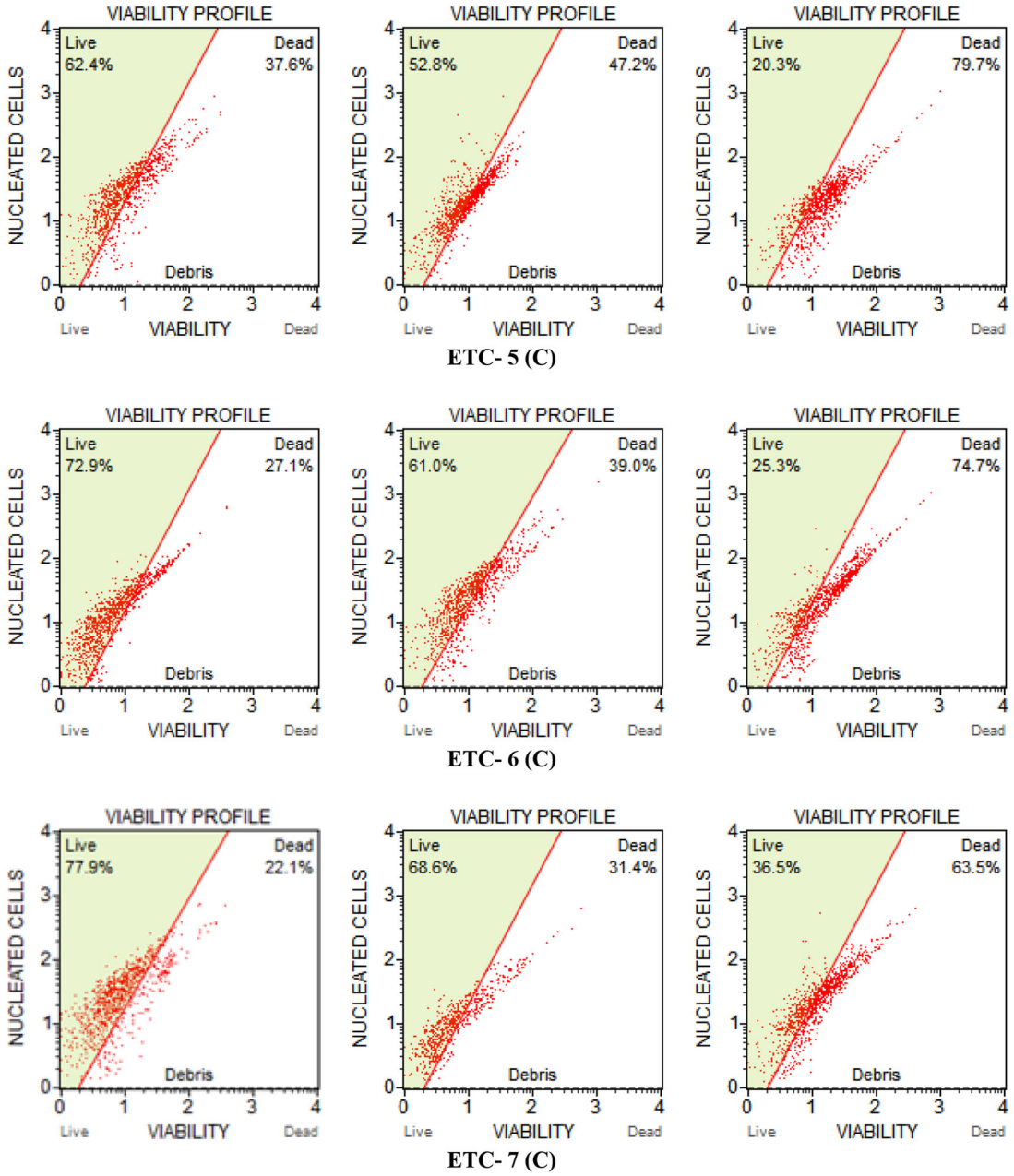


Fig. 9 (continued)

effect of test entities on different *C. albicans* strains was concentration dependent as for control strain *C. albicans* SC5314, cell death ranges from 35.2 to 52.2%, 45.9 to 62.4% and 94.1 to 95.7% at 0.25 × MIC, 0.5 × MIC and 1 × MIC of test compounds, respectively. These figures for fluconazole-susceptible strain *C. albicans* 4175 was 32.0–43.9%, 39.2–60% and 76.3–84.2% and for fluconazole-resistant strain *C. albicans* 5112, the trend for cell death was 22.1–37.6%, 31.4–47.2% and 63.5–79.7% at 0.25 × MIC, 0.5 × MIC and 1 × MIC of test compounds, respectively. These results are in congruent with the MIC results representing ETC-5 as the most effective compound followed by ETC-6 and ETC-7, respectively. To further differentiate the results between the cells and debris and/or non-nucleated cells, cell size index was also done in the same assay and it was confirmed that the results are due to live and dead cells (Fig. S1).

Discussion

The current antifungal therapy is not adequate to treat various invasive fungal infections caused by different emerging multidrug-resistant *Candida* species. Therefore, new antifungal agents with multiple target sites are urgently required. Since ancient times, nature is known for having products of medicinal importance and have been used for the treatment of several diseases (Mushtaq et al. 2018). Despite in-depth studies on natural compounds to develop novel antifungal drugs, very limited have reached the clinical trials or beyond. Therefore, modifying natural compounds to synthesize derivatives/analogues with favourable physicochemical and improved biological properties as well as to lower their side effects is an innovation to discover novel drugs against various fungal diseases including candidiasis (Pan et al. 2013; Liu et al. 2017).

We have previously reported the importance of tosylation in eugenol to improve its antifungal activity (Ahmad et al. 2015). In a separate study, modified novel eugenol tosylate congeners with different functional groups were synthesized and tested against different *C. albicans* isolates (Lone et al. 2019 under review). Modification of these congeners have significantly improved their antifungal activity in comparison to the previous tosylates congeners. In the present study, we selected the three most active novel eugenol tosylate congeners (ETC-5, ETC-6 and ETC-7) and tested their in silico and in vitro effect on ergosterol biosynthesis pathway, which is one of the established drug targets in *C. albicans*. The in silico results displayed that CYP51-ETC-5 complex significantly altered the protein conformation as compared to CYP51-ETC-6 and CYP51-ETC-7. Our results also suggested that the highest structural compactness was observed in CYP51-ETC-5 complex, while higher fluctuations were noted in CYP51-ETC-6 and CYP51-ETC-7 complexes which attributed to the active interaction of CYP51 with ETC-5 inhibitor. RoG follows the same pattern as RMSD and thus could be the indicative of enhanced activity of ETC-5 in comparison with ETC-6 and ETC-7 inhibitors. Results also suggest that ETC-5 is more energetically promising and potential inhibitor than ETC-6 and ETC-7 inhibitors. The high negative values of the binding energies of interaction exhibited by ETC-5 binding as compared with ETC-6 and ETC-7, indicative of more promising binding affinity, which could account for the favorable ligand binding. Additionally, interaction of amino acid residues involved in the active site with ETC-5, ETC-6 and ETC-7 was studied to achieve the understanding of ligand–protein interactions. These estimated energies specify comprehensive molecular level indications that could be beneficial to design a drug by producing improved ligand binding. These calculations are computationally low cost, dynamic, almost completely programmed and implemented in the software.

Based on the in silico results reporting the interaction of test compounds with CYP51 enzyme, we tested in vitro effect of these entities on ergosterol biosynthesis pathway. Our results showed, significant decrease in ergosterol biosynthesis in a dose-dependent manner in both fluconazole-susceptible and resistant strains of *C. albicans*. Up to 65% and 90% decrease in total intracellular sterol content was observed at sub-MIC and MIC values of test compounds, respectively, for fluconazole-susceptible strains. In a similar manner, the decrease in sterol content for fluconazole-resistant strain was up to 51% and 79% at sub-MIC and MIC values, respectively. These results are in corroboration with the previous findings where newly laboratory-based synthesized compounds have been reported to possess antifungal activity by targeting ergosterol biosynthesis pathway (Hata et al. 2010). We also reported eugenol and its derivatives impair ergosterol biosynthesis pathway in *Candida* cells and, therefore, these results can further validate our current findings (Ahmad et al. 2010, 2015). Based on the sharp decline in ergosterol biosynthesis in all the *C. albicans* strains after treatment with the test compounds, we tested the effect of ETCs on *ERG11* gene expression levels. *ERG11* is one of the most important genes in ergosterol biosynthesis pathway and its upregulation is associated with azole drug resistance in *C. albicans* (Oliveira et al. 2014; Sanglard et al. 2003; Xu et al. 2015; Alvarez-Rueda et al. 2016; Sanglard 2016). The inhibition of *ERG11p*, an enzyme encoded by *ERG11* gene, results in accumulation of 14 α-methylated sterols, thus obstructing ergosterol biosynthesis which leads damage to membrane and cellular integrity (Alizadeh et al. 2017), whereas overexpression of *ERG11* leads to increased production of *ERG11p*, it is often related with the azole, polyene and azole-polyene cross-resistances (Eddouzi et al. 2013). From the results, we observed significant downregulation in expression of *ERG11* gene in both fluconazole-susceptible and fluconazole-resistant strains of *C. albicans*. These results are in congruence with previous findings where *ERG11* genes were downregulated in different *Candida* species when treated with natural and semisynthetic compounds (Nakayama et al. 2001; Yu et al. 2012). As expected, upregulation of *ERG11* was observed in fluconazole-resistant *C. albicans* strain after exposed to the fluconazole. These results corroborate the findings observed in sterol quantification assay.

From the cell viability assay results, test compounds at their respective MIC values exhibited up to 95.7% and 79.7% cell death in fluconazole-susceptible and fluconazole-resistant isolates of *C. albicans*, respectively. Our findings demonstrated that these ETCs exhibit fungicidal effect than fungistatic by having killing effect of ≥ 90% at their MIC

values. These results correlate with our previous findings where eugenol, the parent compound for these tosylates, as well as different tosylates congeners have been reported to exhibited fungicidal activity (Ahmad et al. 2010, 2015). These results also indicated the similitude in the antifungal activity between the test compounds and amphotericin B, even though there is no relation between the two groups.

In conclusion, our combined results demonstrated that the improved antifungal effect of these newly synthesized eugenol tosylate congeners (ETC-5, ETC-6 and ETC-7) was ascribed to their capability of having fungicidal effect and to inhibit ergosterol biosynthesis in both fluconazole-susceptible and fluconazole-resistant *C. albicans* strains. These compounds also downregulate *ERG11* gene which is related to ergosterol biosynthesis pathway. Further studies are required to understand these antifungal mechanisms of novel eugenol tosylate congeners and test their ability in animal studies against multidrug-resistant *Candida* species and forms. These studies can provide the development of novel antifungal drugs with multiple modes of antifungal actions, which could play a role in minimising drug resistance in fungal pathogens.

Author contributions Conceived and designed the experiments: AASK. Performed the experiments: SAL. Analyzed the data: SAL, SK, AA. Contributed reagents/materials/analysis tools: AA. Wrote the paper: SAL.

Funding We gratefully acknowledge financial support from University Research Committee Grant for 2019—Friedel Sellschop Award (Grant no: AZMD019), Wits Faculty of Health Sciences Research Committee (FRC, Grant no: 001…5254) and South Africa Medical Research Council (MRC) (Grant no: MLEP016).

Data availability The data that support the findings of this study are available from the corresponding author upon request.

Compliance with ethical standards

Conflict of interest We have no competing interests to declare.

Ethical approval This study was approved by the Human Research Ethics Committee of University of the Witwatersrand (Johannesburg, South Africa). Existing stock cultures of *C. albicans* used in this study were stored in the Department of Clinical Microbiology and Infectious Diseases, University of the Witwatersrand, Johannesburg, South Africa.

References

Ahmad A, Khan A, Manzoor N, Khan LA (2010) Evolution of ergosterol biosynthesis inhibitors as fungicidal against *Candida*. Microb Pathogen 48(1):35–41

Ahmad A, Khan A, Akhtar F, Yousuf S, Xess I, Khan LA, Manzoor N (2011) Fungicidal activity of thymol and carvacrol by disrupting ergosterol biosynthesis and membrane integrity against *Candida*. Eur J Clin Microbiol Infect Dis 30(1):41–50

Ahmad A, Wani MY, Khan A, Manzoor N, Molepo J (2015) Synergistic interactions of Eugenol-tosylate and its congeners with fluconazole against *Candida albicans*. PLoS ONE 10:e0145053

Alizadeh F, Khodavandi A, Zalakian S (2017) Quantitation of ergosterol content and gene expression profile of ERG11 gene in fluconazole-resistant *Candida albicans*. Curr Med Mycol 3(1):13–19

Alvarez-Rueda N, Fleury A, Logé C, Pagniez F, Robert E, Morio F (2016) The amino acid substitution N136Y in *Candida albicans* sterol 14alpha-demethylase is involved in fluconazole resistance. Med Mycol 54(7):764–775

Berman HM, Westbrook J, Feng Z, Gilliland G, Bhat TN, Weissig H, Shindyalov IN, Bourne PE (2000) The protein data bank. Nucleic Acids Res 28(1):235–242

Brown GD, Denning DW, Gow NA, Levitz SM, Netea MG, White TC (2012) Hidden killers: human fungal infections. Sci Transl Med 4:165rv13

Carrasco H, Raimondi M, Svetaz L, Liberto M, Rodriguez MV, Espinoza L, Madrid A, Zacchino S (2012) Antifungal activity of eugenol analogues. Influence of different substituents and studies on mechanism of action. Molecules 17(1):1002–1024

de Oliveira CG, Vilas-Boas LA, Castilho MS, Carazzolle MF, Pirovani CP, Selbach-Schnadelbach A, Gramacho KP, Ramos PI, Barbosa LV, Pereira GA, Góes-Neto A (2014) Analysis of the ergosterol biosynthesis pathway cloning, molecular characterization and phylogeny of lanosterol 14 α-demethylase (ERG11) gene of Moniliophthora perniciosa. Genet Mol Biol 37(4):683–693

Dias DA, Urban S, Roessner U (2012) A historical overview of natural products in drug discovery. Metabolites 2(2):303–336

Eddouzi J, Parker JE, Vale-Silva LA, Coste A, Ischer F, Kelly S, Manai M, Sanglard D (2013) Molecular mechanisms of drug resistance in clinical *Candida* species isolated from Tunisian hospitals. Antimicrob Agents Chemother 57(7):3182–3193

Genheden S, Ryde U (2015) The MM/PBSA and MM/GBSA methods to estimate ligand-binding affinities. Expert Opin Drug Discov 10(5):449–461

Harvey MJ, De Fabritiis G (2009) An implementation of the smooth particle Mesh Ewald Method on GPU hardware. J Chem Theory Comput 5(9):2371–2377

Hata M, Ishii Y, Watanabe E, Uoto K, Kobayashi S, Yoshida K, Otani T, Ando A (2010) Inhibition of ergosterol synthesis by novel antifungal compounds targeting C-14 reductase. Med Mycol 48(4):613–621

Hipólito TMM, Bastos GTL, Barbosa TWL, de Souza TB, Coelho LFL, Dias ALT, Rodríguez IC, Dos Santos MH, Dias DF, Franco LL, Carvalho DT (2018) Synthesis, activity, and docking studies of eugenol-based glucosides as new agents against *Candida sp*. Chem Biol Drug Des 92(2):1514–1524

Keniya MV, Sabherwal M, Wilson RK, Woods MA, Sagatova AA, Tyndall JDA, Monk BC (2018) Crystal structures of full-length lanosterol 14α-demethylases of prominent fungal pathogens *Candida albicans* and *Candida glabrata* provide tools for antifungal discovery. Antimicrob Agents Chemother 62(11):e01134

Lindberg E, Hammarström H, Ataollahy N, Kondori N (2019) Species distribution and antifungal drug susceptibilities of yeasts isolated from the blood samples of patients with candidemia. Sci Rep 9(1):3838

Liu X, Ma Z, Zhang J, Yang L (2017) Antifungal compounds against *Candida* infections from traditional Chinese medicine. Biomed Res Int 2017:4614183

Mushtaq S, Abbasi BH, Uzair B, Abbasi R (2018) Natural products as reservoirs of novel therapeutic agents. EXCLI J 17:420–451

Nakayama H, Nakayama N, Arisawa M, Aoki Y (2001) In vitro and in vivo effects of 14alpha-demethylase (ERG11) depletion in *Candida glabrata*. Antimicrob Agents Chemother 45(11):3037–3045

Pan SY, Zhou SF, Gao SH, Yu ZL, Zhang SF, Tang MK, Sun JN, Ma DL, Han YF, Fong WF, Ko KM (2013) New perspectives on how to discover drugs from herbal medicines: Cam's outstanding contribution to modern therapeutics. Evid Based Complement Alternat Med 2013:627375

Perez A, MacCallum JL, Brini E, Simmerling C, Dill KA (2015) Grid-based backbone correction to the ff12SB protein force field for implicit-solvent simulations. J Chem Theory Comput 11(10):4770–4779

Pettersen EF, Goddard TD, Huang CC, Couch GS, Greenblatt DM, Meng EC, Ferrin TE (2004) UCSF Chimera—a visualization system for exploratory research and analysis. J Comput Chem 25(13):1605–1612

Piccione D, Mirabelli S, Minto N, Bouklas T (2019) Difficult but not impossible: in search of an anti-candida vaccine. Curr Trop Med Rep 6:42–49

Rajput SB, Karuppayil SM (2013) Small molecules inhibit growth, viability and ergosterol biosynthesis in *Candida albicans*. Springerplus 2(1):26

Roe DR, Cheatham TE (2013) PTRAJ and CPPTRAJ: software for processing and analysis of molecular dynamics trajectory data. J Chem Theory Comput 9(7):3084–3095

Sanglard D (2016) Emerging threats in antifungal-resistant fungal pathogens. Front Med (Lausanne) 3:11

Sanglard D, Ischer F, Parkinson T, Falconer D, Bille J (2003) *Candida albicans* mutations in the ergosterol biosynthetic pathway and resistance to several antifungal agents. Antimicrob Agents Chemother 47(8):2404–2412

Sastry GM, Adzhigirey M, Day T, Annabhimoju R, Sherman W (2013) Protein and ligand preparation: parameters, protocols, and influence on virtual screening enrichments. J Comput Aided Mol Des 27(3):221–234

Sievert DM, Ricks P, Edwards JR, Schneider A, Patel J, Srinivasan A, Kallen A, Limbago B, Fridkin S, National Healthcare Safety Network (NHSN) Team, and Participating NHSN Facilities (2013) Antimicrobial-resistant pathogens associated with healthcare-associated infections: summary of data reported to the National Healthcare Safety Network at the Centers for Disease Control and Prevention, 2009–2010. Infect Control Hosp Epidemiol 34(1):1–14

Silva FFM, Monte FJQ, Lemos TLG, Nascimento PGG, Costa AKM, Paiva LMM (2018) Eugenol derivatives: synthesis, characterization, and evaluation of antibacterial and antioxidant activities. Chem Cent J 12(1):34

Trott O, Olson AJ (2010) AutoDock Vina: improving the speed and accuracy of docking with a new scoring function, efficient optimization, and multithreading. J Comput Chem 31(2):455–461

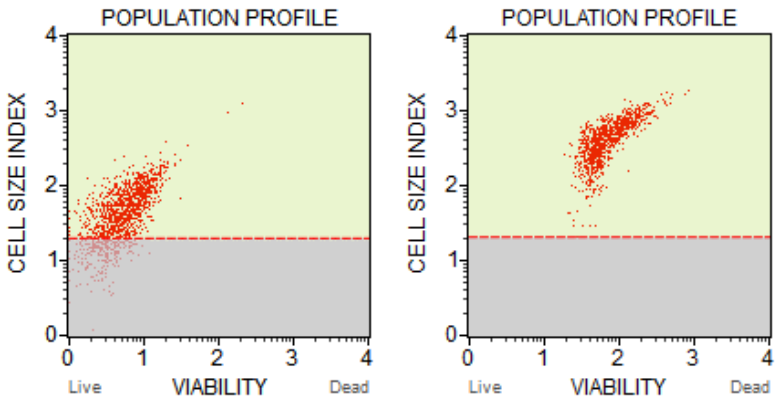
van der Spoel D, van Maaren PJ (2006) The origin of layer structure artifacts in simulations of liquid water. J Chem Theory Comput 2(1):1–11

Xu Y, Sheng F, Zhao J, Chen L, Li C (2015) ERG11 mutations and expression of resistance genes in fluconazole-resistant *Candida albicans* isolates. Arch Microbiol 197(9):1087–1093

Yu LH, Wei X, Ma M, Chen XJ, Xu SB (2012) Possible inhibitory molecular mechanism of farnesol on the development of fluconazole resistance in *Candida albicans* biofilm. Antimicrob Agents Chemother 56(2):770–775

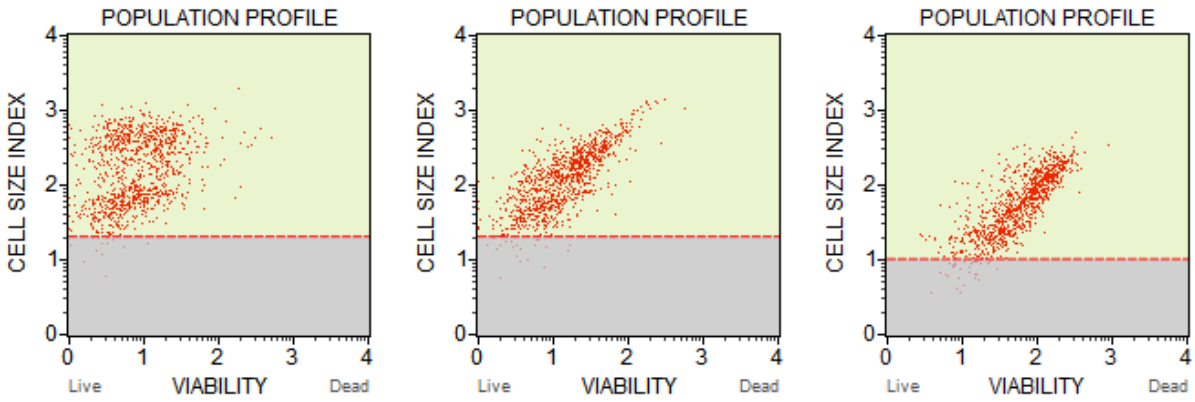
Publisher's Note Springer Nature remains neutral with regard to jurisdictional claims in published maps and institutional affiliations.

SUPPLEMENTARY DATA:

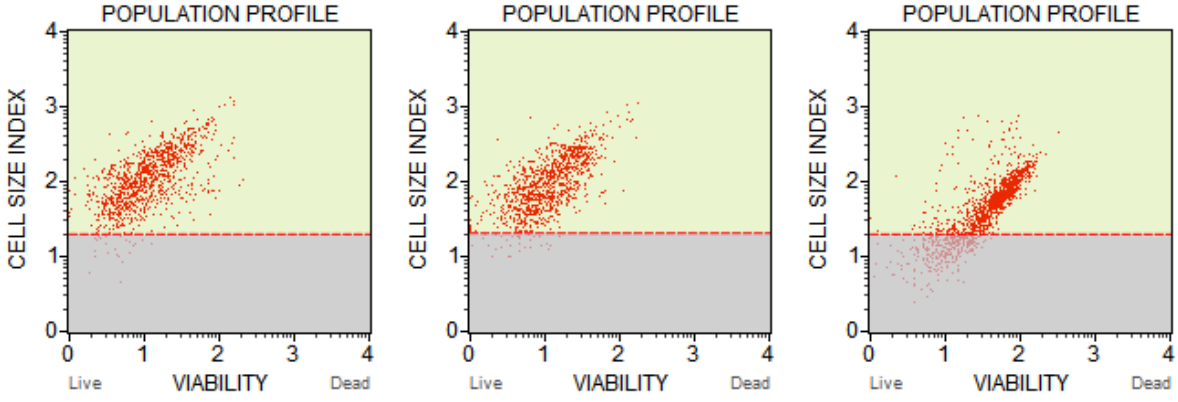


Negative Control **Positive Control**

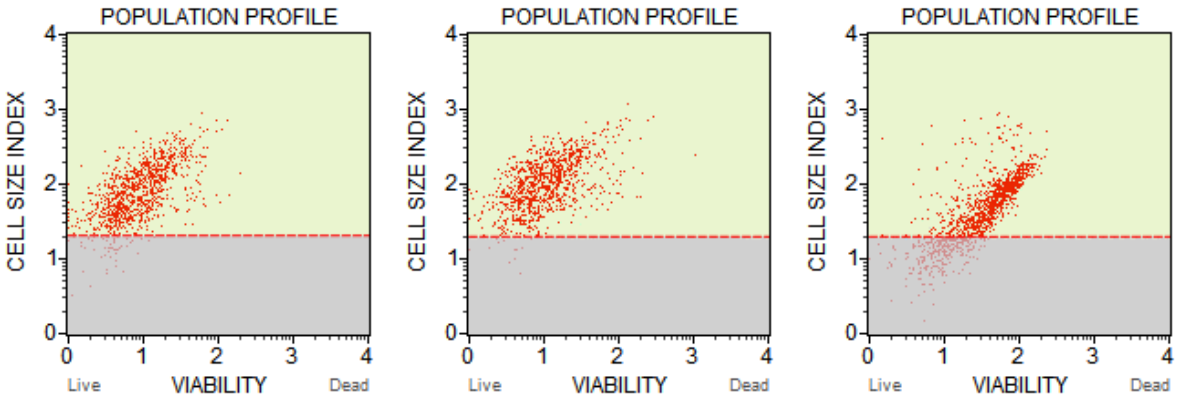
0.25 × MIC **0.5 × MIC** **1 × MIC**



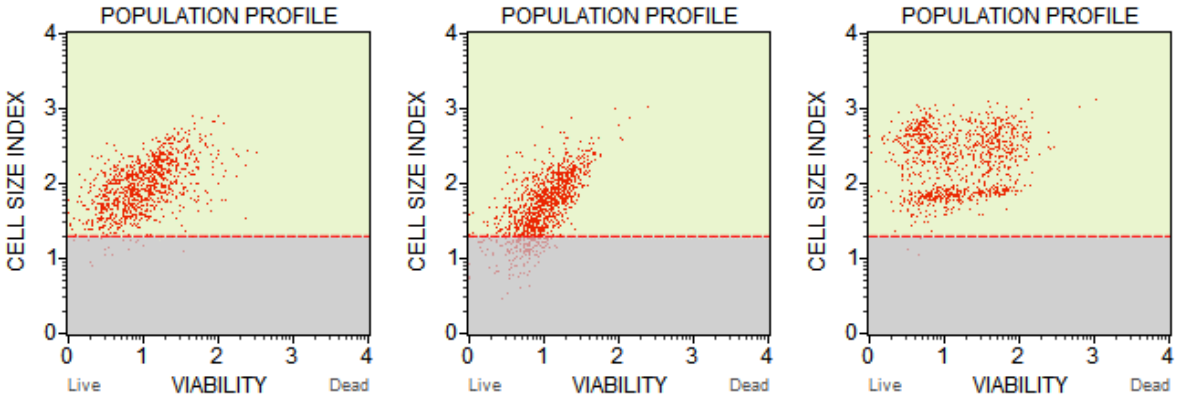
ETC- 5 (A)



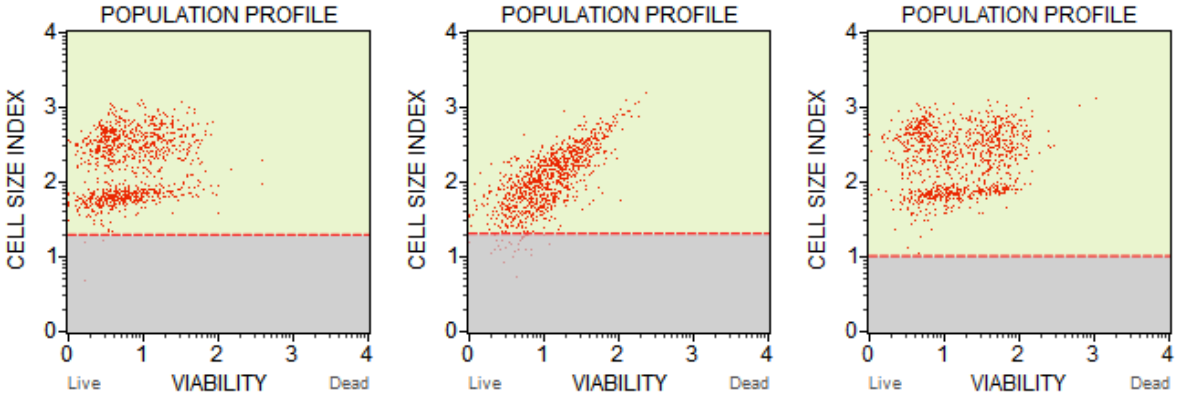
ETC- 6 (A)



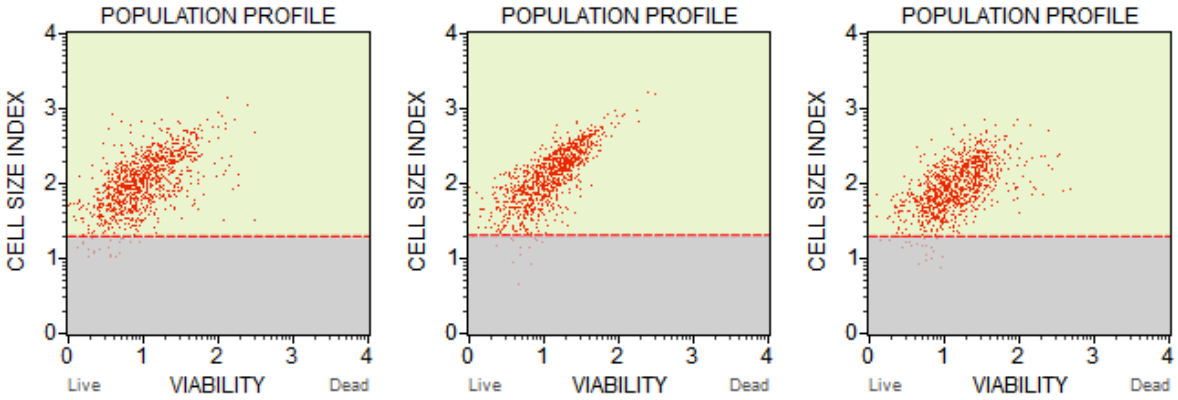
ETC- 7 (A)



ETC- 5 (B)



ETC- 6 (B)



ETC- 7 (B)

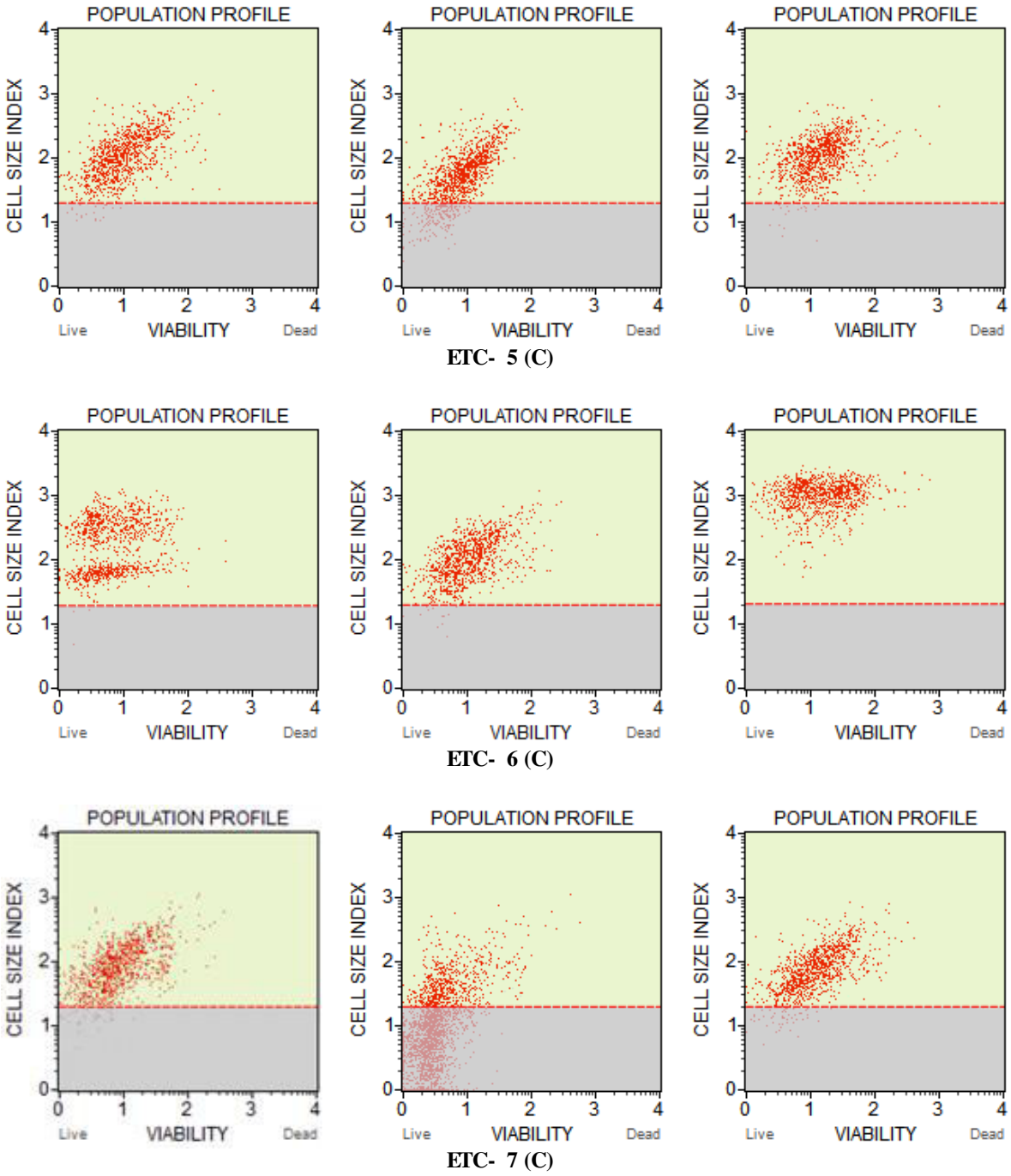


Fig. S1 Cell Viability assay for *Candida* cells: Cells at a density of 1 × 10^7 treatment to 0.25 × MIC, 0.5 × MIC and 1 × MIC of the test compounds (ETC-5, ETC-6 and ETC-7) and cell viability assay was performed by the Muse Count & Viability reagent (Millipore) following the manufacturer's protocols. A, B, C represents control strain *C. albicans* SC5314, fluconazole susceptible *C. albicans* 4175, and fluconazole resistant *C. albicans* 5112 respectively. Negative and positive controls represent untreated and heat killed cells respectively.